THE JOURNAL OF BIOLOGICAL CHEMISTRY VOL. 285, NO. 46, pp. 36179–36187, November 12, 2010

The Hyposensitive N187D P2X7 Mutant Promotes Malignant Progression in Nude Mice*

Received for publication, April 1, 2010, and in revised form, August 19, 2010 Published, JBC Papers in Press, September 13, 2010, DOI 10.1074/jbc.M110.128488

Jing-Hui Chong[‡§], Guo-Guang Zheng[‡§1], Yuan-Yuan Ma[‡], Hai-Yan Zhang[‡], Kun Nie[‡], Yong-Min Lin[‡§], and Ke-Fu Wu[‡]

From the [‡]State Key Laboratory of Experimental Hematology, Institute of Hematology and Blood Diseases Hospital, Chinese Academy of Medical Sciences and Peking Union Medical College, 288 Nanjing Road, Tianjin 300020, China and the [§]Center for Stem Cell Medicine, Chinese Academy of Medical Sciences, Beijing 100730, China

Nucleotides are new players in the intercellular communication network. P2X7 is a member of the P2X family of receptors, which are ATP-gated plasma membrane ion channels with diverse biological functions. Abnormal expression and dysfunction of P2X7 have been reported in leukemias. Here, we report a new P2X7 mutant (an A^{559}-to-G substitution causing N187D P2X7) cloned from J6-1 leukemia cells. The characteristics of N187D P2X7 were studied by establishing stably transfected K562 cell lines. Our results show that N187D P2X7 required a higher concentration of agonist for its activation, leading to Ca^{2+} influx (EC_{50} = 293.3 ± 6.6 μM for the mutant and 93.6 ± 2.2 μM for wild-type P2X7) and ERK phosphorylation, which were not caused by differential cell-surface expression or related to high ATPase activity on the cell surface and in the extracellular space. K562 cells expressing this N187D mutant showed a proliferative advantage and reduced pro-apoptosis effects *in vitro* and *in vivo*. Furthermore, elevated angiogenesis and CD206-positive macrophage infiltration were found in tumor tissues formed by K562-M cells. In addition, higher expression of VEGF and MCP1 could be detected in tumor tissues formed by K562-M cells. Our results suggest that N187D P2X7, representing mutants hyposensitive to agonist, might be a positive regulator in the progression of hematopoietic malignancies.

The survival and functions of cells are tightly modulated by intercellular communication in multicell organisms. Abnormal communication leads to dysfunction of cells and various kinds of diseases. For decades, peptide signal molecule-mediated intercellular communication has been well established. Nucleotides have been proposed as a ubiquitous family of extracellular signaling molecules mediating intercellular communication (1).

P2 purinoreceptors consist of P2X and P2Y family receptors. P2X receptors, characterized by two transmembrane domains with both intracellular N and C termini, are ATP-gated plasma membrane ion channels that mediate transmembrane cation fluxes (2). Seven distinct subtypes (P2X1–P2X7) have been cloned and identified in mammalian cells. P2X7 is unique for the longest C-terminal intracellular domain and bifunctional response upon stimulation, *i.e.* exposure to ATP or the more potent agonist BzATP[2] renders P2X7 permeable to Na^+, K^+, and Ca^{2+}, whereas repeated or prolonged application of either agonist induces the formation of a cytolytic pore, which is permeable to larger cations such as positively charged ethidium.

P2X7 receptors are widely distributed in a variety of cell types and are involved in diverse biological effects. A sustained high level of extracellular ATP was detected in a tumor environment (3), which implied the involvement of abnormal signaling mediated by P2 family receptors. In fact, an abnormal high expression of the P2X7 receptor was observed in solid tumors (4, 5) as well as in hematopoietic malignancies, such as B-cell chronic lymphocytic leukemia (6), acute leukemia, and myelodysplastic syndromes (7, 8), etc. Moreover, a series of P2X7 polymorphisms have been discovered, and their impacts on P2X7 functions, mechanisms, and relationship with diseases were studied in a number of variants. Among them, several loss-of-function polymorphisms, including 1513A→C (E496A) (9), 1729T→A (I568N) (10), 946G→A (R307Q) (11), and 1096C→G (T357S) (12), and a 5′-intronic splice site polymorphism (13) were reported with diverse mechanisms, including influence of pore formation (14), failure of its trafficking to the cell surface (10), and abolishment of ATP binding (11). In addition, a gain-of-function polymorphism, 489C→T (H155Y) from human chronic lymphocytic leukemia lymphocytes, was characterized with elevated calcium influx and ethidium bromide uptake functions (15). Nevertheless, the involvement of these polymorphisms or mutants in pathogenesis was still obscure. The focused studies on A1513C P2X7 reached controversial conclusions (16, 17).

Our previous work demonstrated the high expression of P2X7 in leukemia patients and the lack of P2X7-mediated calcium response in the J6-1 leukemia cell line upon BzATP stimulation at regular concentrations (7). Then, the entire coding region of P2X7 was cloned from this cell line, and DNA sequencing analysis revealed a substitution of A^{559} with G, causing an N187D substitution (18). How this mutation confers

* This work was supported by Grants 30470897 and 30971111 from the National Natural Science Foundation of China and Grants 2009CB918901 and 2009CB521803 from the Major State Basic Research Development Program (973 Program) of China and Grant 2010DFB30270 from the Ministry of Science and Technology of China and Grant 09ZCZDSF03800 from Tianjin Science and Technology Key Program.

[1] To whom correspondence should be addressed: State Key Laboratory of Experimental Hematology, Inst. of Hematology and Blood Diseases Hospital, Chinese Academy of Medical Sciences and Peking Union Medical College, 288 Nanjing Rd., Tianjin 300020, China. Tel.: 86-22-2390-9053; Fax: 86-22-2390-9032; E-mail: zhengggtjchn@yahoo.com.cn.

[2] The abbreviations used are: BzATP, benzoyl-ATP; PE, phycoerythrin; TAM, tumor-associated macrophage.

dysfunction to P2X7 and its possible role in malignancies were of interest. In this study, we found that N187D P2X7 needed higher levels of agonist for activation. In addition, K562 cells bearing this hyposensitive mutant showed a proliferative advantage over wild-type P2X7 *in vitro* and in a nude mouse model. Furthermore, elevated angiogenesis and CD206-positive macrophage infiltration could be detected in tumor tissues formed by K562 cells bearing this mutant.

EXPERIMENTAL PROCEDURES

Cell Lines, Cell Culture, and Antibodies—The K562 leukemia cell line was maintained in our laboratory. All cells were cultured in RPMI 1640 medium supplemented with 10% FBS (Invitrogen) and antibiotics in a humidified atmosphere of 5% CO_2 at 37 °C. All culture supplies were screened and selected on the basis of being endotoxin-free. Anti-P2X7 and FITC-conjugated anti-P2X7 polyclonal antibodies, recognizing the C-terminal and extracellular parts of P2X7, respectively, were purchased from Sigma. Antibodies against ERK (C-16), JNK (C-17), and p38 (N-20) were from Santa Cruz Biotechnology. The phospho-MAPK family antibody sampler kit was a product of Cell Signaling Technology. FITC-conjugated anti-mouse F4/80 (BM8), Alexa Fluor-conjugated anti-mouse CD206 (MR5D3), and phycoerythrin (PE) Q5-conjugated anti-mouse CD31 (390) polyclonal antibodies were from BioLegend.

Plasmid Construction, Transfection Procedures, and Gain of Polyclones—A pTARGET vector carrying wild-type P2X7 (pTARGET-wP2X7) was constructed from pTARGET-mP2X7 (with an A^{559}-to-G mutation), which was previously cloned in our laboratory from the J6-1 leukemia cell line, by an overlap PCR method for base substitution mutagenesis using the following primers: forward 1, 5′-ATA TCT CGA GCA GGG AGG GAG GCT GTC-3′; reverse 1, 5′-CAC AGT GAA GT**T** TTC GGC ACT G-3′; forward 2, 5′-CAG TGC CGA A**A**A CTT CAC TGT G-3′; and reverse 2, 5′-AGG TGG TAC CGG TGC CTG GCT TCA GTA AG-3′ (GenBank™ accession number NM_002562).

The PCR product was digested with XhoI and KpnI and cloned into the pTARGET vector containing a selective marker (*neo*, the neomycin phosphotransferase gene). The construct was verified by DNA sequencing and purified using a plasmid purification kit (TaKaRa). K562 cells were then transfected with pTARGET-mP2X7 (K562-M), pTARGET-wP2X7 (K562-W), or a blank vector (K562-V) using Lipofectamine 2000 reagent (Invitrogen) following the manufacturer's instructions. After 48 h, the medium was changed to fresh RPMI 1640 medium containing 600 μg/ml G418 (Invitrogen) in 24-well plates. Stable polyclones expressing P2X7 were verified by RT-PCR, Western blotting, flow cytometry, and confocal microscopy.

RT-PCR—Total RNA from cells or tumor tissues was extracted using TRIzol reagent (Invitrogen) following the manufacturer's instructions, and cDNA was subsequently synthesized using Moloney murine leukemia virus reverse transcriptase (Promega). Semiquantitative RT-PCR was performed using a GeneAmp PCR System 2400 thermocycler (PerkinElmer Life Sciences) for verification of stable transfectants using the following primers: 5′-TCT GCA AGA TGT CAA GGG C-3′ and 5′-TCA CTC TTC GGA AAC TCT TTC C-3′ for P2X7 (GenBank™ accession number NM_002562), 5′-GGT GGA GAG GCT ATT CGG CT-3′ and 5′-GAT AGA AGG CGA TGC GCT GC-3′ for the *neo* gene (accession number AY540613), and 5′-TGA AGG TCG GAG TCA ACG GAT TTG G-3′ and 5′-CAT GTG GGC CAT GAG GTC CAC CAC-3′ for GAPDH (accession number NM_002046).

Quantitative real-time PCR was performed using an ABI Prism 7500 sequence detector (Applied Biosystems) with the following primers: 5′-TGC ACC CAC GAC AGA AGG-3′ and 5′-GCA CAC AGG ACG GCT TGA-3′ for murine VEGF (accession number NM_001025250), 5′-CAC TTG AAG GGT GGA GC-3′ and 5′-GGG CTA AGC AGT TGG TG-3′ for murine GAPDH (accession number NM_008084), 5′-CCA TGA ACT TTC TGC TGT CTT-3′ and 5′-ATC GCA TCA GGG GCA CAC AG-3′ for human VEGF (accession number NM_001025366), 5′-CTT CTG TGC CTG CTG CTC-3′ and 5′-GCT GCT GGT GAT TCT TCT AT-3′ for murine MCP1 (monocyte chemoattractant protein 1; accession number NM_002982), and 5′-GAA GGT GAA GGT CGG AGT C-3′ and 5′-GAA GAT GGT GAT GGG ATT TC-3′ for human GAPDH (accession number NM_002046).

Flow Cytometry Analysis of Stably Transfected K562 Polyclones—Cells were blocked with 2% normal goat serum (Sigma) for 0.5 h and stained with FITC-conjugated anti-P2X7 antibody recognizing the extracellular part of P2X7 for 1 h at 4 °C before undergoing flow cytometry analysis (FACSCalibur, BD Biosciences). Isotype controls were included.

Cell Proliferation Assay—Cells were seeded at a concentration of 3×10^4 in 96-well plates for 24, 48, 72, and 96 h before the addition of 3-(4,5-dimethylthiazol-2-yl)-2,5-diphenyltetrazolium bromide for the cell proliferation assay. Results were validated by cell counting.

Apoptosis Assay and Flow Cytometry Analysis—For apoptosis analysis, cells were cultured at 5×10^4 cells/ml in the presence or absence of various concentrations of BzATP. The percentage of apoptotic cells was evaluated using an annexin V-PE kit (BD Biosciences) according to the manufacturer's protocol. Apoptotic cells were analyzed by flow cytometry (FACSCalibur) using CellQuest software.

Colony Formation Assay—Colony formation was carried out in triplicate in 100 μl of essential medium (2×10^3 cells/ml) containing 1% methylcellulose, 20% FCS, 700 μg/ml G418, 5×10^{-4} mol/L β-mercaptoethanol, and 0.03% glutamine in 96-well culture plates for 7 days. Colonies (containing 40 or more cells) were counted under a reversed microscope. Three independent experiments were carried out.

Measurement of ATPase Activity—ATPase activity was determined as the enzymatic release of P_i from ATP into medium as described previously (19). Cells in log phase were washed twice and resuspended in the testing buffer (20 mM HEPES, 150 mM NaCl, 10 mM glucose, and 2 mM $CaCl_2$ (pH 7.5)) at a concentration of 1.0×10^6 cells/ml. ATP was added to a final concentration of 1 mM, and samples were incubated for 20 min at 37 °C. Subsequently, the cells were sedimented, and the amount of P_i in the supernatant was determined by mixing an equal volume of reaction mixture with ice-cold P_i reagent consisting of 1% (w/v) ammonium molybdate, 1% (w/v) SDS, and 0.2% (w/v) ascorbic acid in 3% (v/v) H_2SO_4. After color

development for 15 min at 37 °C, the absorbance at 820 nm was measured using a Beckman DU-70 spectrophotometer (20). Two values, non-enzymatic P_i release from ATP into the medium during incubation without cells and P_i content in the cell-containing samples without the addition of ATP, were subtracted from the total P_i release, giving values for the enzymatic ATP hydrolysis. KH_2PO_4 was used as P_i standard. The specific activity is expressed as nmol of $P_i/10^6$ cells/min.

Measurements of Intracellular Free Ca^{2+}—The intracellular free Ca^{2+} concentration ($[Ca^{2+}]_i$) was determined using the fluorescent indicator fura-2/AM (8). Briefly, cells were incubated with 3 μM fura-2/AM at 37 °C for 20 min before being washed twice with Locke's solution and then resuspended. The cell suspension was placed in the thermostat-regulated sample chamber of a dual excitation beam spectrophotometer (F-4500, Hitachi, Tokyo, Japan) with continuous stirring. The fluorescence intensities at 510 nm were recorded when excited at 340 and 380 nm simultaneously. BzATP was added to the final concentrations needed. At the end of each measurement, Triton X-100 was added to obtain maximal fluorescence, and then excess EDTA was added to obtain minimal fluorescence. $[Ca^{2+}]_i$ was calculated using F-4500 intracellular cation measurement system software (Version 1.02). In blocking experiments, the P2X7 receptor antagonist KN62 was preincubated with cells for 0.5 h before $[Ca^{2+}]_i$ analysis.

Western Blotting—Cells were collected by centrifugation and lysed for 15 min on ice in cell lysis buffer (Cell Signaling Technology). The detergent-insoluble material was then removed by centrifugation at 12,000 rpm for 15 min at 4 °C. Twenty microliters of lysates with equal amounts of proteins were collected from each vial and mixed with 2× reducing buffer (40% (w/v) glycerol, 9.2% (w/v) SDS, 250 mmol/liter Tris (pH 6.8), 20% (w/v) β-mercaptoethanol, and 0.04% bromphenol blue) for electrophoresis on 10% SDS-polyacrylamide gels before blotting onto nitrocellulose membrane.

The membrane was blocked with 5% nonfat milk in TBST (150 mmol/liter NaCl, 25 mmol/liter Tris, and 0.1% Tween 20 (pH 7.5)) for 2 h at room temperature. After incubations with primary antibodies overnight at 4 °C and with horseradish peroxidase-conjugated secondary antibodies for 2 h at room temperature, visualization was carried out by an enhanced chemiluminescence method using ECL Western blotting detection reagents (Pierce) according to the manufacturer's instructions. Membrane was washed three times with TBST between every two steps. All bands were quantified using AlphaEaseFC 4.0 software, and the ratio of the phosphorylated band to its native band was defined as its phosphorylation level.

Tumor Growth in Nude Mice—Female BALB/c nude mice, which were 6 week olds, were purchased from the Center for Experimental Animals, Academy of Military Medical Sciences. The immunodeficient mice were housed in sterile microisolators. After irradiation with Cs-137 at 400 centigrays, nude mice were injected subcutaneously on the dorsal side with 1.5×10^7 K562-V, K562-W, or K562-M cells in a volume of 200 μl. After ~6 days, when the tumors were palpable, the length and width of each tumor were measured with metric calipers. The tumor volume was then calculated using the following equation: volume = (length × width × width)/2 mm^3. Mice were killed on day 21.

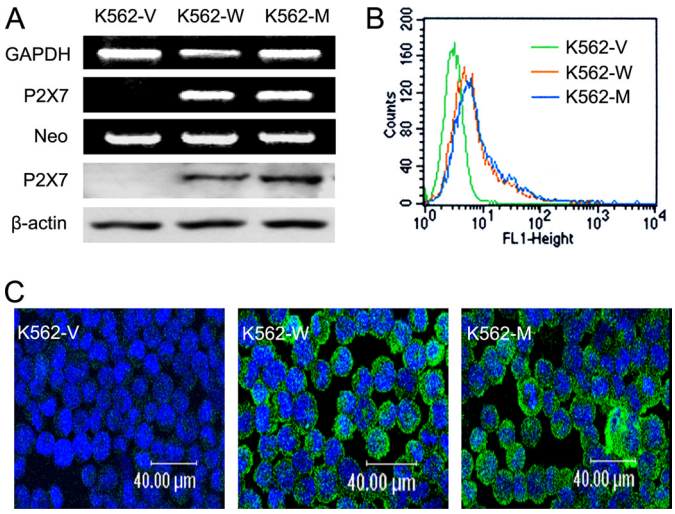

FIGURE 1. **Establishment of K562 cell lines stably expressing P2X7.** K562 leukemia cells were transfected with a blank, wild-type P2X7-expressing, or N187D P2X7-expressing vector. Stably transfected polyclones (K562-V, K562-W, and K562-M) were obtained by G418 selection. *A*, *upper*, their successful establishment were confirmed by RT-PCR using primers for either P2X7 or the *neo* gene. GAPDH was used as an internal control. *Lower*, the expression of P2X7 in the cells was detected by Western blotting as described under "Experimental Procedures." β-Actin was used as an internal control. *B*, flow cytometry analysis of membrane P2X7 levels was performed using FITC-labeled polyclonal antibodies against the extracellular part of P2X7. *C*, confocal microscopy analysis of P2X7 expression was performed using FITC-labeled polyclonal antibodies against the C-terminal part of P2X7.

Confocal Microscopy—The formalin-fixed, paraffin-embedded tissue sections (8 μm) were deparaffinized and rehydrated in PBS. Antigen retrieval was performed by heating the sections in 0.01 mol/liter citrate buffer in a microwave oven. Frozen tissue sections (5 μm) were fixed with cold acetone for 10 min at room temperature. Nonspecific binding was blocked by incubating the tissue sections with 2% normal goat serum in PBS for 20 min. Slides were then incubated with FITC-conjugated anti-mouse F4/80 and Alexa Fluor-conjugated anti-mouse CD206 antibodies or with PE Q5-conjugated anti-mouse CD31 antibody at a dilution of 1:100 at room temperature for 30 min. All samples were washed three times with PBS, and then nuclei were stained using DAPI (Sigma). To detect P2X7 expression in K562 cell lines, cell smears were stained with anti-P2X7 antibody, followed by FITC-labeled goat anti-rabbit secondary antibodies. Apoptotic cells on paraffin-embedded tissue slides were stained using the DeadEnd™ fluorometric TUNEL system (Promega) following the manufacturer's instructions. The specimens were mounted in 80% glycerin/PBS solution and analyzed by confocal scanning microscopy (Leica TCS SP).

Statistical Analysis—Two-tailed Student's *t* test was used to determine the difference between two independent groups. Analysis was done using the SPSS software package. Significance was accepted when the *p* values were <0.05.

RESULTS

Establishment of K562 Cell Lines Stably Expressing Wild-type or Mutant P2X7—K562 cells without endogenous P2X7 expression were transfected with the wild-type and mutant P2X7-expressing vectors or with the blank vector before undergoing G418 selection. The stably transfected polyclones were designated K562-W, K562-M, and K562-V, respectively, after

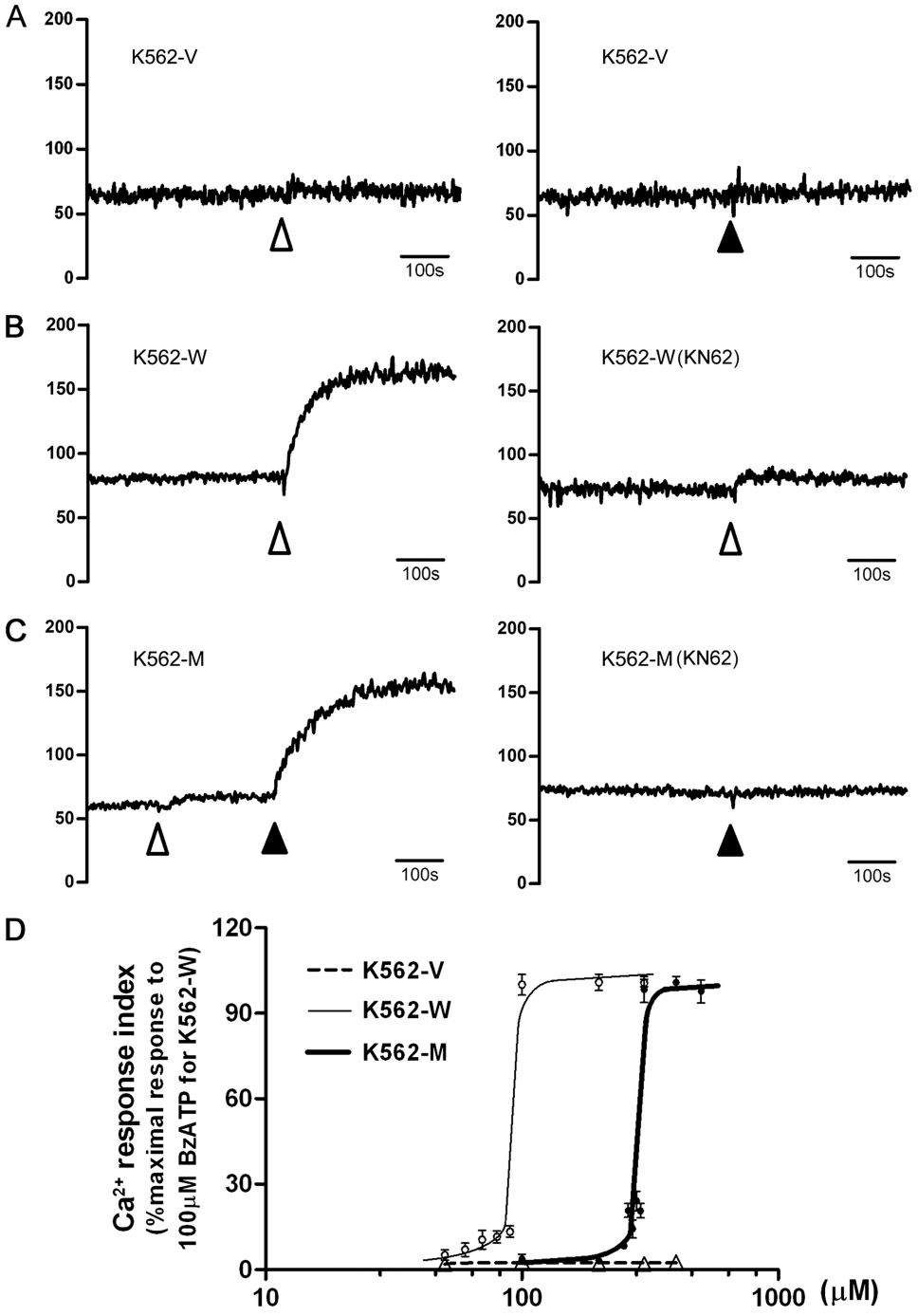

FIGURE 2. **P2X7-specific calcium response in transfected cells.** *A–C*, P2X7 receptor function in transfected cell lines was studied by detecting the cytoplasmic free calcium ($[Ca^{2+}]_i$) with the specific agonist BzATP using a Hitachi F-4500 spectrophotometer with fura-2/AM. BzATP was added at the time points indicated to a final concentration of 100 μM (△) or 300 μM (▲). In blocking experiments, KN62 was preincubated with cells for 0.5 h before $[Ca^{2+}]_i$ analysis. $[Ca^{2+}]_i$ (nM) is shown on the *y axis*. The time scale of 100 s is indicated. *D*, calcium response influx is expressed as a percentage of the maximal response to 100 μM BzATP in K562-W cells, which was defined as 100% response. The curves shown were calculated by nonlinear regression analysis. Data represent the typical results from at least three independent experiments.

verification by RT-PCR, Western blotting (Fig. 1*A*), flow cytometry (Fig. 1*B*), and confocal microscopy (Fig. 1*C*).

N187D P2X7 Requires a Higher Concentration of Agonist for Its Activation—A P2X7-specific calcium response could be observed upon stimulation by either its natural ligand, ATP, or its most specific and complete agonist, BzATP. As ATP is also an agonist for other P2X family receptors or P2Y family receptors, we mainly monitored $[Ca^{2+}]_i$ upon BzATP stimulation. Upon stimulation with 100 μM BzATP (regular level), a sustained increase in $[Ca^{2+}]_i$ could be observed in K562-W cells, which could be blocked by the P2X7-specific antagonist KN62 (Fig. 2*B*). In contrast, no $[Ca^{2+}]_i$ increase could be observed in K562-M cells (Fig. 2*C*). However, when the concentration of BzATP was increased to 300 μM, an increase in $[Ca^{2+}]_i$ could be observed in K562-M cells, which could also be blocked by KN62 pretreatment (Fig. 2*C*). No calcium response could be observed in K562-V cells (Fig. 2*A*). The dose-dependent effect of BzATP on the calcium response demonstrated that the EC_{50} values for K562-W and K562-M cells were 93.6 ± 2.2 and 293.3 ± 6.6 μM, respectively (Fig. 2*D*). These data suggest that N187D P2X7 needs a higher level of agonist for its activation.

The activation of MAPK pathways is an important downstream event for P2X7 (21). The activation of ERK, JNK and p38 MAPK signal pathways was investigated in these cells for a further understanding of N187D P2X7. The results showed that upon stimulation with 100 or 300 μM BzATP, the activation of ERK (but not JNK or p38) could be observed in K562-W cells, whereas activation of ERK could only be detected at a higher concentration of agonist in K562-M cells (Fig. 3*A*). These effects were dose-dependent: an obvious activation of ERK1/2 could be detected at 100 μM and higher concentrations in K562-W cells, whereas it could be observed at 200 μM and higher concentrations in K562-M cells (Fig. 3*B*). These effects mediated by wild-type and mutant P2X7 and could be blocked by pretreatment with either the MEK inhibitor U0126 or the P2X7 antagonist KN62 (Fig. 3, *C* and *D*). These data strengthen the observation that N187D P2X7 is hyposensitive to its ligand.

As high E-ATPase can cause rapid hydrolyzation of ATP, leading to low extracellular ATP levels for P2X7 activation, the ATPase activities of K562-V, K562-W, and K562-M cells were studied, and the results showed that they had similar levels of ATPase activity (Fig. 4*A*).

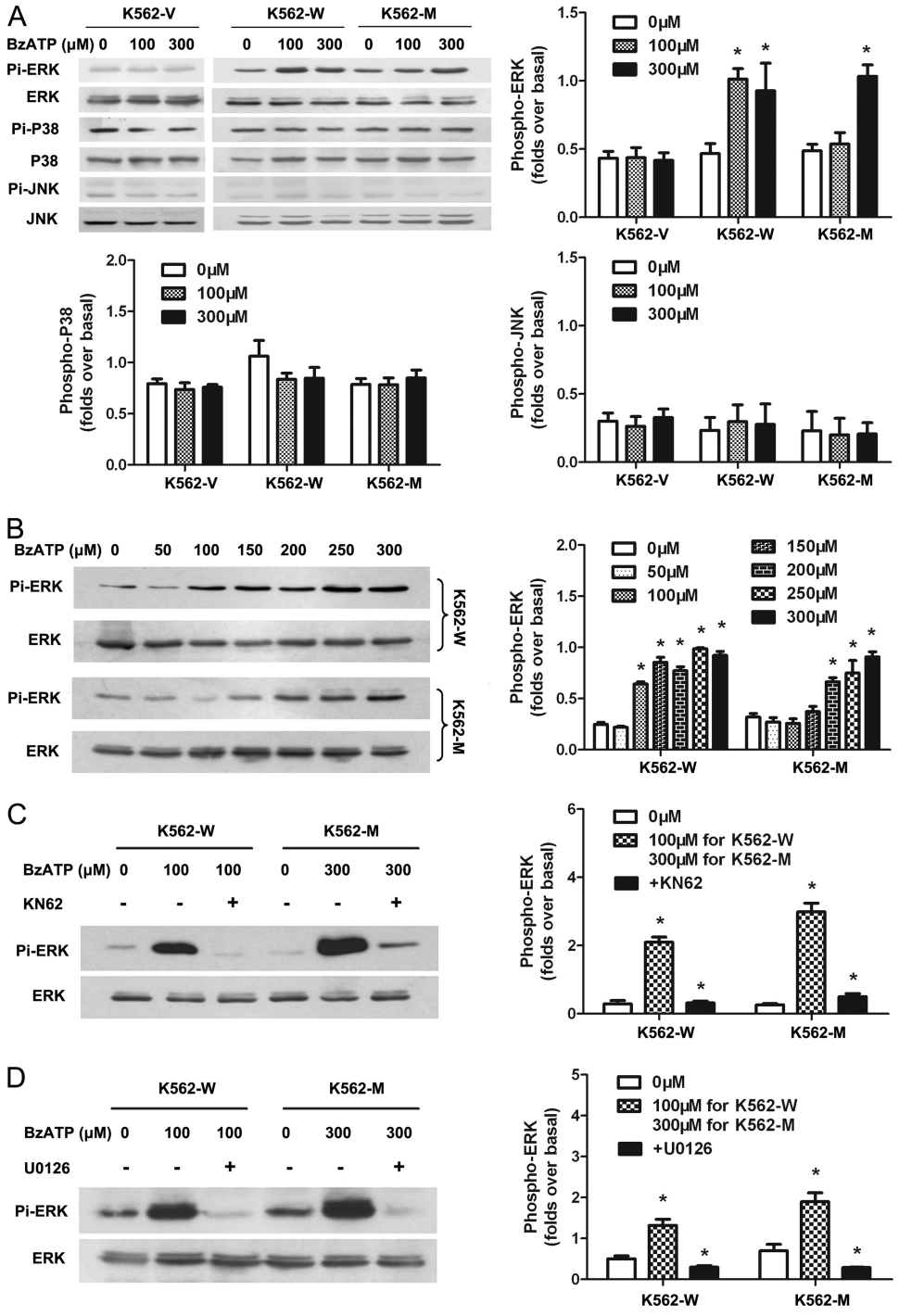

FIGURE 3. **P2X7-specific activation of MAPK signal pathways in transfected cells.** *A*, the P2X7-mediated activation of ERK, JNK, and p38 MAPK signal pathways in K562-V, K562-W, and K562-M cells was studied by Western blotting 5 min post-stimulation by 100 or 300 μM BzATP as described under "Experimental Procedures." Antibodies recognizing their native proteins were used as internal controls. *B*, the dose-dependent effects of agonist on the activation of ERK1/2 in K562-W and K562-M cells were studied using different final concentrations of BzATP as indicated. *C*, cells were pretreatment with KN62 before stimulation by BzATP. *D*, cells were pretreatment with the MEK inhibitor U0126 before stimulation by BzATP. The relative phosphorylation intensities were quantified using AlphaEaseFC 4.0 software.

In Vitro Proliferation and Apoptosis Characteristics of Transfected K562 Cells—To investigate the potential involvement of N187D P2X7 in the regulation of leukemia cells, we compared the *in vitro* growth characteristics of the three cell lines by means of proliferation, apoptosis, and colony formation assays. The results showed that the proliferation potential of K562-M cells was significantly higher than that of K562-V or K562-W cells ($p < 0.01$ at 24 h and $p < 0.001$ at 48 h and thereafter) (Fig. 4*B*). K562-M cells showed a reduced apoptosis rate upon regular BzATP stimulation compared with K562-W cells (Fig. 4*C*). In a colony-forming assay, K562-M cells not only formed more colonies (Fig. 4*D*) but also formed larger colonies compared with K562-W cells (Fig. 4*E*). These data suggest that leukemia cells bearing this P2X7 mutant have a greater growth potential compared with those bearing either wild-type P2X7 or the blank control vector. Different polyclones showed similar results.

Oncogenicity of Transfected Cells in Vivo—To study the *in vivo* effects of N187D P2X7, BALB/c nude mice were subcutaneously implanted with the same amount of K562-V, K562-W, or K562-M cells. Palpable tumors could be detected 6 days post-inoculation. The size of each tumor was measured with metric calipers every 2 days. At an early stage, no difference in tumor progression among the three cell lines was observed. Then, the tumor progression of K562-M cells was much faster compared with K562-V or K562-W cells (Fig. 5*A*). Nude mice were killed on day 21. The size of the tumors formed by K562-M cells was significantly bigger compared with those formed by K562-W or K562-V cells (Fig. 5*B*). The weight of K562-M tumors was significantly heavier than that of K562-V or K562-W tumors (Fig. 5*C*). Different polyclones were used in such experiments, and similar results were obtained.

The hematoxylin/eosin staining results showed no significant difference among tumor samples. Necrosis could be observed in the middle of the tumor tissues. Tumor cells undergoing mitosis were frequently observed. Tumor cells were closely packed, with scant cytoplasm, prominent nuclear membranes, and large nuclei. However, the apoptosis analysis of tumor tissues indicated that the tumors formed by K562-M cells had significantly reduced apoptotic cells compared with those formed by K562-W cells (Fig. 6*A*).

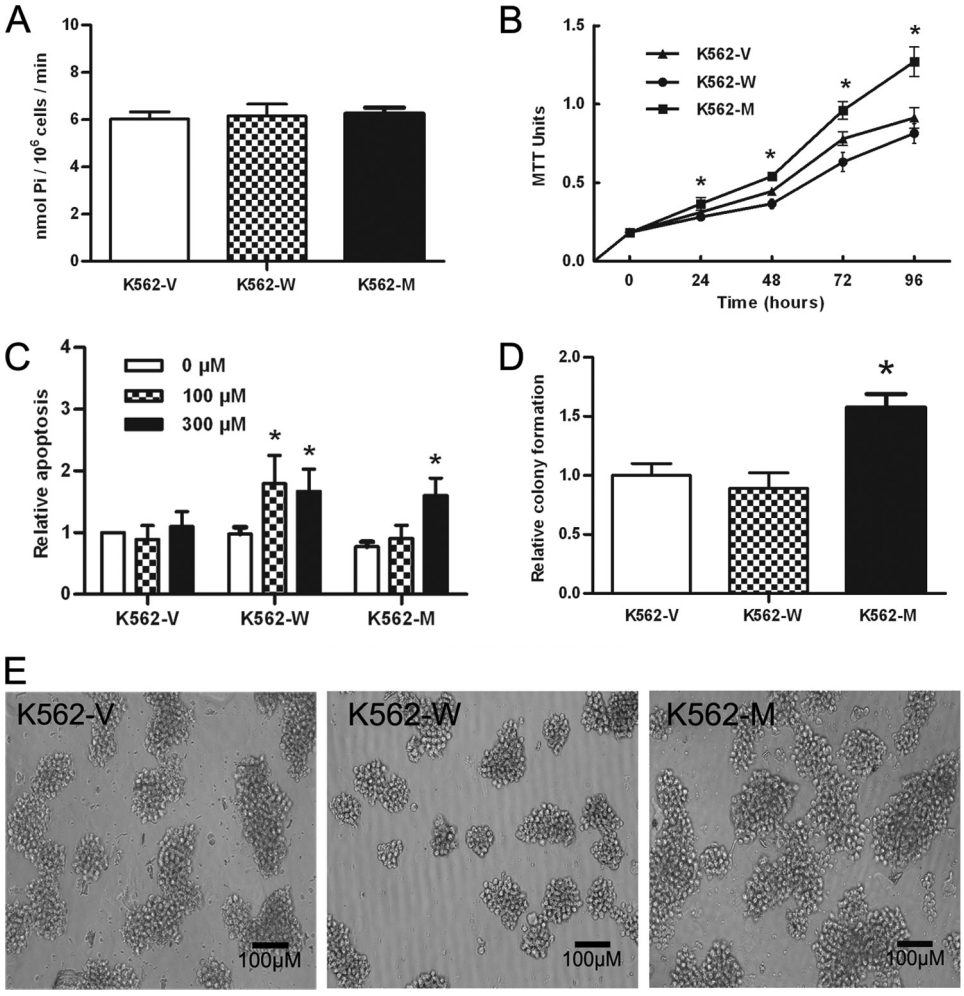

FIGURE 4. ***In vitro* characteristics of K562-V, K562-W, and K562-M cells.** *A*, the cell surface and extracellular space ATPase activity in three cell lines was analyzed by molybdate assay and is expressed as nmol of $P_i/10^6$ cells/min. *B*, the cell proliferation potential in liquid culture was determined by the 3-(4,5-dimethylthiazol-2-yl)-2,5-diphenyltetrazolium bromide (*MTT*) method at time points indicated. *C*, cell apoptosis was studied at 24 h post-stimulation by BzATP at the concentrations indicated using an annexin V-PE kit. The relative apoptosis index is shown as the -fold apoptosis rates in K562-V cells without BzATP stimulation. *D* and *E*, the colony-forming potential was analyzed by a colony-forming assay. The relative colony formation index (*D*) is shown as the -fold colony rates in K562-V cells. Colonies under a microscope are also shown (*E*). *, $p < 0.05$ by Student's *t* test.

Elevated Angiogenesis in Tumor Tissues Formed by K562-M Cells—High level angiogenesis is associated with tumor progression (22). Hence, we analyzed the vessel density in these tumor tissues using PE Q5-conjugated anti-CD31 antibody. A high density of vessels was found in tumor tissues formed by K562-M cells but not in those formed by K562-V or K562-W cells (Fig. 6*B*). Quantitative analysis (performed by counting the vessel number under a confocal microscope) indicated a significant increase of vessel density in K562-M compared with K562-W cells (Fig. 6*B*, *right*). To further determine the pro-angiogenic mechanism, the expression of VEGF, basic FGF, and hepatocyte growth factor pro-angiogenic factors was measured using both mouse- and human-specific primers by real-time RT-PCR. Although no difference was found among cultured K562-V, K562-W, and K562-M cells, the levels of human and mouse VEGF (but not basic FGF or hepatocyte growth factor) in tumor tissues formed by K562-M cells were higher than those in K562-V (2.7- and 3.0-fold) or K562-W (2.2- and 3.5-fold) tissues, suggesting that microenvironment-related complex mechanism(s) was involved in the *in vivo* process.

Elevated Macrophage Infiltration in K562-M Tumor Tissues—The fact that mouse VEGF was elevated in K562-M tumor tissues suggested that mouse cells might contribute to tumor progression in this model. As macrophages are important for the development of tumors (23), we studied the distribution of macrophages in these samples using the macrophage-specific marker anti-F4/80 antibody. Confocal microscopy analysis showed that a few macrophages were found in K562-V or K562-W tumor tissues, whereas a remarkable increase in macrophage infiltration occurred in K562-M tumor tissues (Fig. 6*C*).

Infiltrating macrophages in tumor tissues can be taught to become tumor-associated macrophages (TAM), which play important roles in tumor progression. CD206 (24) is a surface marker of alternatively activated macrophages (M2 macrophages), and its high level expression in TAMs has been reported. We thus studied the expression of CD206 in infiltrating macrophages by dual-color immunofluorescence staining. The results showed that a large proportion of macrophages coexpressed CD206 in K562-M tumor tissues, whereas a small proportion of macrophages were double-positive in K562-V or K562-W tumor tissues (Fig. 6*C*).

We further detected the expression level of MCP1, which plays important roles in recruiting monocytes to tumor sites. The results indicated that K562-M tumor tissues had a higher level of human MCP1 compared with K562-V (3.0-fold) or K562-W (3.6-fold) tumor tissues, whereas no difference was found among these cultured cells. No difference was detected for mouse MCP1 in tumor tissues.

DISCUSSION

Among P2X family receptors, P2X7 is unique for the longest C-terminal intracellular domain. Although abnormal expression (7, 8) and several polymorphisms leading to dysfunction (9–11) were studied in malignancies, and different alternative splicing variants (25) were reported, its significance in diseases has not been fully established. Up to now, several loss-of-function polymorphisms and a gain-of-function polymorphism have been reported, and different mechanisms have been sug-

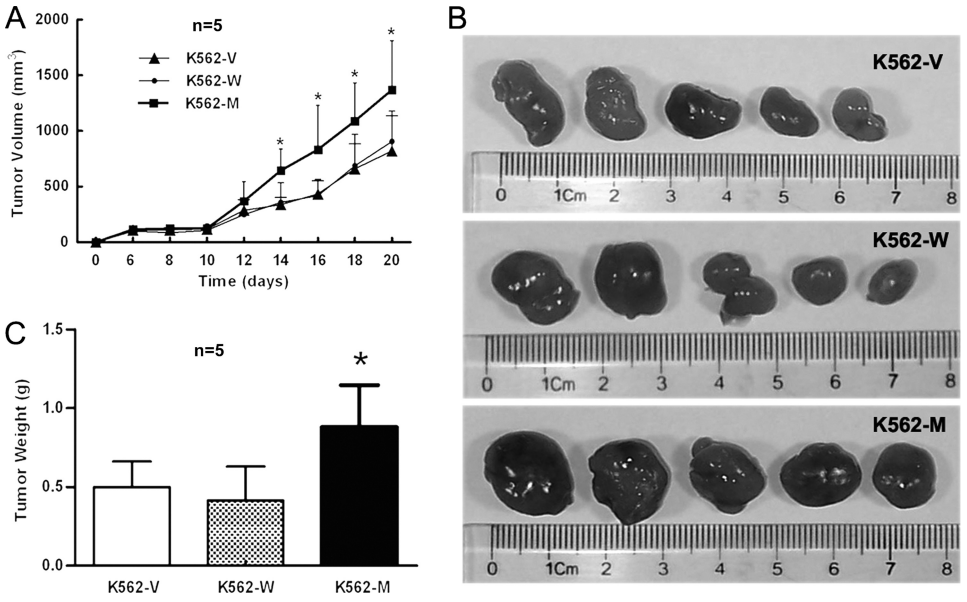

FIGURE 5. **Oncogenicity of K562-V, K562-W, and K562-M cells in a nude mouse model.** *A*, female BALB/c nude mice (five per group) were injected subcutaneously on day 0 with 1.5×10^7 K562-V/K562-W/K562-M cells, and the tumor size was measured on the dates indicated. The size of each tumor from the groups was pooled. *B*, shown is the size of the tumors formed by three cells on day 21. *C*, shown is the weight of the tumors formed by these cells on day 21. Different polyclones were used, and typical results are shown. *, $p < 0.05$ by Student's *t* test.

gested. Here, we have reported a new P2X7 mutant, N187D P2X7, with unique dysfunction features.

The characteristics of N187D P2X7 were studied in this work by establishing K562 cell lines expressing either N187D or wild-type P2X7, as the parental K562 cell line lacks P2X7 expression. The calcium response and the activation of MAPK pathways are the two main downstream events after P2X7 activation. Furthermore, it was reported that P2X7-mediated MAPK cascade activation and calcium influx were independent downstream events (26). We observed here that an increase in $[Ca^{2+}]_i$ could be detected in K562-W cells upon stimulation with a regular concentration of agonists (BzATP), whereas it could be detected in only K562-M cells at a higher level of

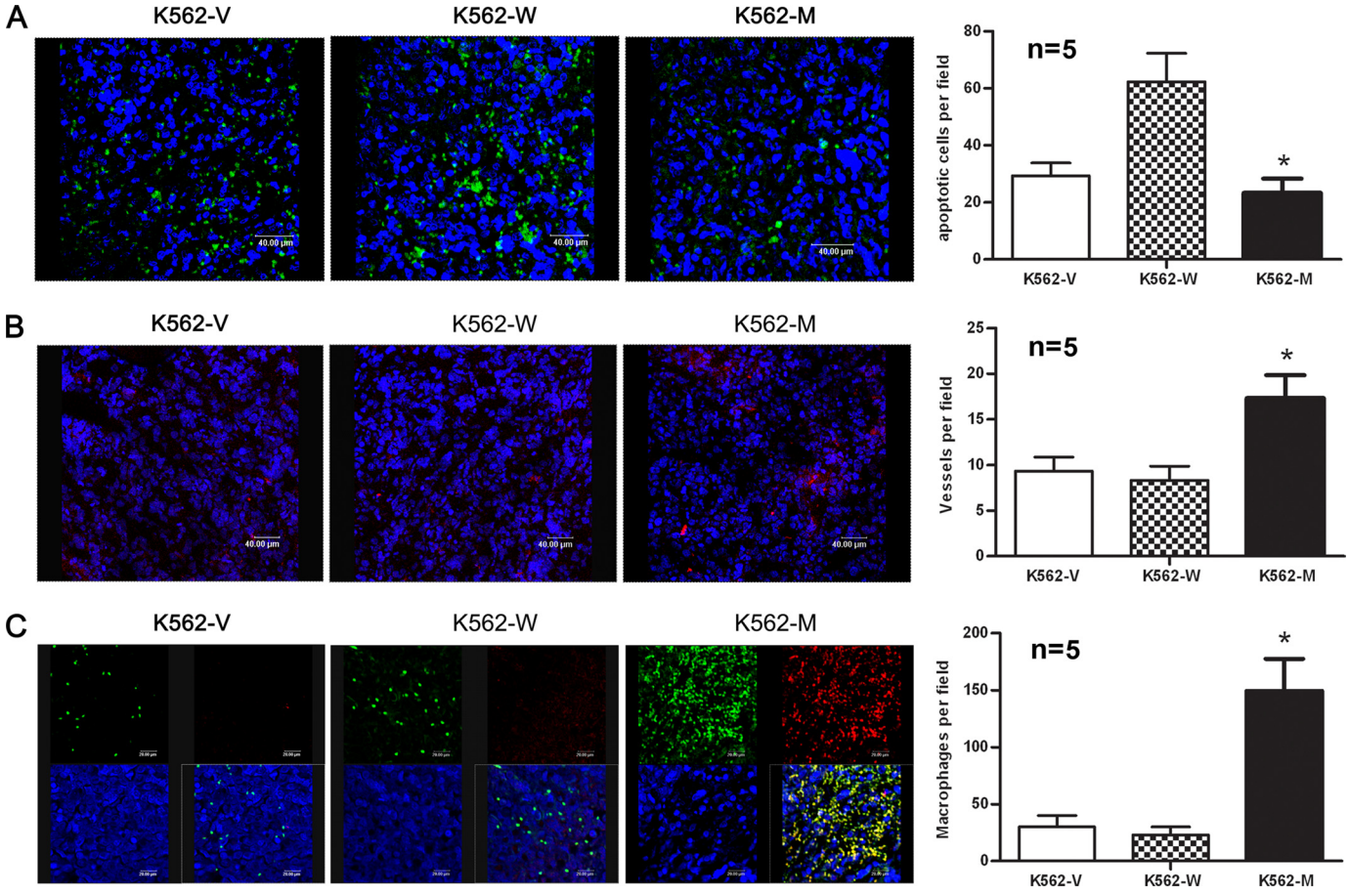

FIGURE 6. **Tumor tissue analysis.** Sections were obtained from nude mouse tumor tissues formed by K562-V, K562-W, and K562-M cells on day 21 for confocal analysis. *A*, apoptotic cells in paraffin-embedded tumor sections were stained using the DeadEnd™ fluorometric TUNEL system. *B*, vessels in frozen tumor sections were stained with PE-conjugated anti-mouse CD31 antibody. *C*, macrophages in tumor sections were stained with FITC-conjugated anti-mouse F4/80 and Alexa Fluor-conjugated anti-mouse CD206 antibodies. Quantitative analysis of apoptotic cells, vessel density, and macrophages was performed by counting 10 random high power fields from five different tumor samples within each group, and the results are shown on the right. *, $p < 0.05$ by Student's *t* test.

agonists. Further evidence indicated a much higher EC_{50} for N187D P2X7 compared with wild-type P2X7. Similar results were also observed in the activation of the ERK MAPK pathway. Furthermore, no difference was observed for the expression level and membrane localization of N187D mutant and wild-type P2X7 in transfected cells. Moreover, the ATPase activity on the cell surface and extracellular space of these cells, which might cause a quick hydrolysis of extracellular ATP to a level under the threshold for P2X7 activation, showed no significant difference. These results suggest that N187D P2X7 might be hyposensitive to agonist for its activation.

Studies (11, 27, 28) on the molecular structure and ATP-binding site of P2X7 provided important clues to answer the question at to how the substitution affected the sensitivity of mutant P2X7 to its ligand. The binding site was believed to be located within the extracellular loop of P2X7, and positively charged amino acids, such as lysine, were suggested to be important for ATP binding by interacting with the phosphate groups of the ATP molecule. It was reported that the ATP-binding site of the P2X7 receptor, which was structurally similar to class II aminoacyl-tRNA synthetases, was located in an antiparallel six-stranded β-pleated sheet formed by Phe^{188}–Val^{321} (27). Furthermore, two positively charged residues, Lys^{193} and Lys^{311}, have been identified in human P2X7 to be essential for ATP binding (28). Asn^{187} is located at the edge of the first β-pleated sheet and near the putative ATP-binding site (Lys^{193}). The substitution of Asn with Asp will bring a more negative charge to the binding pocket, which may affect the binding of ATP. In addition, as Asn^{187} is conserved and glycosylated, more evidence is needed to determine whether the presence of glycosylation has positive roles in ATP binding.

The effects of N187D P2X7 on cell proliferation were also studied. The K562-M cells showed a significantly higher proliferative advantage *in vitro* and oncogenicity *in vivo*. As P2X7 activation leads to cell apoptosis, the mechanism seems to be simple, as described previously (29). In fact, the reduced pro-apoptosis effects of the N187D mutant were observed *in vitro*, and fewer apoptotic cells were detected in tumor tissues formed by K562-M cells. However, our additional work demonstrated that other complex mechanisms might contribute to the rapid progression of K562-M tumor tissues *in vivo*. Angiogenesis plays pivotal roles in tumor progression (30). Tumor tissues formed by K562-M cells showed higher angiogenesis compared with two controls. The analysis of several pro-angiogenic factors showed that the elevated expression of VEGF (both mouse and human origin) could be detected in K562-M tumor tissues, suggesting that both tumor cells and mouse cells contributed to the high angiogenesis.

Macrophages play important roles in tumor progression (31), and abnormal activated macrophages in a tumor environment can secrete a wide range of pro-angiogenic factors (32, 33). Thus, infiltrating macrophages were analyzed. A remarkable increase in infiltrating macrophages, which coexpressed CD206, was observed in K562-M tumor tissues. CD206 is a marker of alternatively activated macrophages (M2 macrophages) and was reported to be expressed by TAMs. Increasing evidence has demonstrated that TAMs play important roles in tumor cell survival, proliferation, invasion, metastasis, and angiogenesis in tumor tissues (33). Hence, the results suggest that abnormal activated macrophages might play important roles in the progression of tumors formed by K562-M cells in this nude mouse model. For a better understanding of the infiltrating process, the expression of MCP1 was studied, and a higher level was found in K562-M tumors. As VEGF was also reported to stimulate migration of macrophages (34, 35), several factors might cooperatively contribute to the process.

Although abnormal expression and dysfunction of P2X7 have been reported in malignancies, the mechanisms of this receptor or its mutants in the progression of malignancies have not been established. Here, we have suggested that, in addition to apoptosis, other aspects and complex mechanisms should be considered. In our model, the expression of VEGF and MCP1 was up-regulated in cells expressing N187D P2X7 in tumor development through unknown mechanisms. High levels of malignant cell-derived MCP1 and VEGF resulted in the recruitment of macrophages. Then, the infiltrating macrophages were taught to become TAMs. In turn, the TAMs began to form an environment favorable for tumor growth, including a high level of mouse VEGF. Finally, the tumor environment plays positive roles in tumor development by stimulating the growth of tumor cells and promoting angiogenesis.

Our results suggest that complex mechanisms should be considered to understand P2X7 in the progression of malignancies. Our observations provide clues toward understanding such P2X7 mutations leading to hyposensitive dysfunction in hematologic malignancies or solid tumors.

Acknowledgments—We thank Mei Zhang and Hai-Rong Jia for technical help. We also gratefully acknowledge Dr. Hongmin Li (Wadsworth Center) for helpful discussion on the potential influence of the mutant structure of P2X7 on binding activities.

REFERENCES

1. Burnstock, G. (1997) *Neuropharmacology* **36,** 1127–1139
2. Valera, S., Hussy, N., Evans, R. J., Adami, N., North, R. A., Surprenant, A., and Buell, G. (1994) *Nature* **371,** 516–519
3. Pellegatti, P., Raffaghello, L., Bianchi, G., Piccardi, F., Pistoia, V., and Di Virgilio, F. (2008) *PLoS One* **3,** e2599
4. Solini, A., Cuccato, S., Ferrari, D., Santini, E., Gulinelli, S., Callegari, M. G., Dardano, A., Faviana, P., Madec, S., Di Virgilio, F., and Monzani, F. (2008) *Endocrinology* **149,** 389–396
5. Slater, M., Danieletto, S., Gidley-Baird, A., Teh, L. C., and Barden, J. A. (2004) *Histopathology* **44,** 206–215
6. Adinolfi, E., Melchiorri, L., Falzoni, S., Chiozzi, P., Morelli, A., Tieghi, A., Cuneo, A., Castoldi, G., Di Virgilio, F., and Baricordi, O. R. (2002) *Blood* **99,** 706–708
7. Zhang, X. J., Zheng, G. G., Ma, X. T., Yang, Y. H., Li, G., Rao, Q., Nie, K., and Wu, K. F. (2004) *Leuk. Res.* **28,** 1313–1322
8. Chong, J. H., Zheng, G. G., Zhu, X. F., Guo, Y., Wang, L., Ma, C. H., Liu, S. Y., Xu, L. L., Lin, Y. M., and Wu, K. F. (2010) *Biochem. Biophys. Res. Commun.* **391,** 498–504
9. Gu, B. J., Zhang, W., Worthington, R. A., Sluyter, R., Dao-Ung, P., Petrou, S., Barden, J. A., and Wiley, J. S. (2001) *J. Biol. Chem.* **276,** 11135–11142
10. Wiley, J. S., Dao-Ung, L. P., Li, C., Shemon, A. N., Gu, B. J., Smart, M. L., Fuller, S. J., Barden, J. A., Petrou, S., and Sluyter, R. (2003) *J. Biol. Chem.* **278,** 17108–17113
11. Gu, B. J., Sluyter, R., Skarratt, K. K., Shemon, A. N., Dao-Ung, L. P., Fuller, S. J., Barden, J. A., Clarke, A. L., Petrou, S., and Wiley, J. S. (2004) *J. Biol. Chem.* **279,** 31287–31295

12. Shemon, A. N., Sluyter, R., Fernando, S. L., Clarke, A. L., Dao-Ung, L. P., Skarratt, K. K., Saunders, B. M., Tan, K. S., Gu, B. J., Fuller, S. J., Britton, W. J., Petrou, S., and Wiley, J. S. (2006) *J. Biol. Chem.* **281,** 2079–2086
13. Skarratt, K. K., Fuller, S. J., Sluyter, R., Dao-Ung, L. P., Gu, B. J., and Wiley, J. S. (2005) *FEBS Lett.* **579,** 2675–2678
14. Boldt, W., Klapperstück, M., Büttner, C., Sadtler, S., Schmalzing, G., and Markwardt, F. (2003) *Am. J. Physiol. Cell Physiol.* **284,** C749–C756
15. Cabrini, G., Falzoni, S., Forchap, S. L., Pellegatti, P., Balboni, A., Agostini, P., Cuneo, A., Castoldi, G., Baricordi, O. R., and Di Virgilio, F. (2005) *J. Immunol.* **175,** 82–89
16. Thunberg, U., Tobin, G., Johnson, A., Söderberg, O., Padyukov, L., Hultdin, M., Klareskog, L., Enblad, G., Sundström, C., Roos, G., and Rosenquist, R. (2002) *Lancet* **360,** 1935–1939
17. Nückel, H., Frey, U. H., Dürig, J., Dührsen, U., and Siffert, W. (2004) *Eur. J. Haematol.* **72,** 259–263
18. Nie, K., Zheng, G. G., Lin, Y. M., Zhang, X. J., Wang, L., Song, Y. H., and Wu, K. F. (2006) *Zhonghua Xue Ye Xue Za Zhi* **27,** 602–605
19. Dzhandzhugazyan, K. N., Kirkin, A. F., Thor Straten, P., and Zeuthen, J. (1998) *FEBS Lett.* **430,** 227–230
20. Filippini, A., Taffs, R. E., Agui, T., and Sitkovsky, M. V. (1990) *J. Biol. Chem.* **265,** 334–340
21. Erb, L., Liao, Z., Seye, C. I., and Weisman, G. A. (2006) *Pflugers Arch.* **452,** 552–562
22. Albini, A., Tosetti, F., Benelli, R., and Noonan, D. M. (2005) *Cancer Res.* **65,** 10637–10641
23. Pollard, J. W. (2004) *Nat. Rev. Cancer* **4,** 71–78
24. Mills, C. D., Kincaid, K., Alt, J. M., Heilman, M. J., and Hill, A. M. (2000) *J. Immunol.* **164,** 6166–6173
25. Cheewatrakoolpong, B., Gilchrest, H., Anthes, J. C., and Greenfeder, S. (2005) *Biochem. Biophys. Res. Commun.* **332,** 17–27
26. Amstrup, J., and Novak, I. (2003) *Biochem. J.* **374,** 51–61
27. Freist, W., Verhey, J. F., Stühmer, W., and Gauss, D. H. (1998) *FEBS Lett.* **434,** 61–65
28. Worthington, R. A., Smart, M. L., Gu, B. J., Williams, D. A., Petrou, S., Wiley, J. S., and Barden, J. A. (2002) *FEBS Lett.* **512,** 43–46
29. Di Virgilio, F., Chiozzi, P., Falzoni, S., Ferrari, D., Sanz, J. M., Venketaraman, V., and Baricordi, O. R. (1998) *Cell Death Differ.* **5,** 191–199
30. Folkman, J. (1992) *Semin. Cancer Biol.* **3,** 65–71
31. Wang, L., Zheng, G. G., Ma, C. H., Lin, Y. M., Zhang, H. Y., Ma, Y. Y., Chong, J. H., and Wu, K. F. (2008) *Cancer Res.* **68,** 5639–5647
32. Lewis, C. E., and Pollard, J. W. (2006) *Cancer Res.* **66,** 605–612
33. Crowther, M., Brown, N. J., Bishop, E. T., and Lewis, C. E. (2001) *J. Leukocyte Biol.* **70,** 478–490
34. Clauss, M., Gerlach, M., Gerlach, H., Brett, J., Wang, F., Familletti, P. C., Pan, Y. C., Olander, J. V., Connolly, D. T., and Stern, D. (1990) *J. Exp. Med.* **172,** 1535–1545
35. Leek, R. D., Hunt, N. C., Landers, R. J., Lewis, C. E., Royds, J. A., and Harris, A. L. (2000) *J. Pathol.* **190,** 430–436